International Journal of Nanomedicine

Dovepress
open access to scientific and medical research

Open Access Full Text Article

ORIGINAL RESEARCH

Low molecular weight chitosan nanoparticulate system at low N:P ratio for nontoxic polynucleotide delivery

This article was published in the following Dove Press journal:
International Journal of Nanomedicine
12 March 2012
Number of times this article has been viewed

Mohamad Alameh
Diogo DeJesus
Myriam Jean
Vincent Darras
Marc Thibault
Marc Lavertu
Michael D Buschmann
Abderrazzak Merzouki

Institute of Biomedical Engineering, Department of Chemical Engineering, École Polytechnique, Montréal, Canada

Abstract: Chitosan, a natural polymer, is a promising system for the therapeutic delivery of both plasmid DNA and synthetic small interfering RNA. Reports attempting to identify the optimal parameters of chitosan for synthetic small interfering RNA delivery were inconclusive with high molecular weight at high amine-to-phosphate (N:P) ratios apparently required for efficient transfection. Here we show, for the first time, that low molecular weight chitosan (LMW-CS) formulations at low N:P ratios are suitable for the in vitro delivery of small interfering RNA. LMW-CS nanoparticles at low N:P ratios were positively charged (ζ-potential ~20 mV) with an average size below 100 nm as demonstrated by dynamic light scattering and environmental scanning electron microscopy, respectively. Nanoparticles were spherical, a shape promoting decreased cytotoxicity and enhanced cellular uptake. Nanoparticle stability was effective for at least 20 hours at N:P ratios above two in a slightly acidic pH of 6.5. At a higher basic pH of 8, these nanoparticles were unravelled due to chitosan neutralization, exposing their polynucleotide cargo. Cellular uptake ranged from 50% to 95% in six different cell lines as measured by cytometry. Increasing chitosan molecular weight improved nanoparticle stability as well as the ability of nanoparticles to protect the oligonucleotide cargo from nucleases at supraphysiological concentrations. The highest knockdown efficiency was obtained with the specific formulation 92-10-5 that combines sufficient nuclease protection with effective intracellular release. This system attained >70% knockdown of the messenger RNA, similar to commercially available lipoplexes, without apparent cytotoxicity. Contrary to previous reports, our data demonstrate that LMW-CS at low N:P ratios are efficient and nontoxic polynucleotide delivery systems capable of transfecting a plethora of cell lines.

Keywords: siRNA, nonviral delivery system, chitosan, gene silencing, RecQL1, ApoB

Introduction

RNA interference (RNAi), an evolutionary endogenous gene regulation mechanism based on double-stranded RNA (short hairpin RNA, microRNA, Piwi-interacting RNA, and small interfering RNA [siRNA]), has provided a potential new class of therapeutics.[1] Since its discovery in *Caenorhabditis elegans*,[2] RNAi has been proven effective in mammalian cells[1,3–11] and has reached clinical trials.[1,12–14] However, direct delivery of RNAi-inducing entities such as synthetic siRNA or short hairpin RNA continues to be problematic owing to their rapid extracellular/intracellular degradation by nucleases (ie, RNAse and DNAse), limited blood stability, poor cellular uptake, and nonspecific targeting.[15–17] As a consequence, the translation of RNAi into a clinical therapeutic reality is still pending resolution of these issues.

Correspondence: Abderrazzak Merzouki
Institute of Biomedical Engineering, Department of Chemical Engineering, École Polytechnique, PO Box 6079, Station Centre-ville, Montréal (Québec), Canada H3C 3A7
Tel +1 514 340 5121 ext 4799
Fax +1 514 340 5227
Email abderrazzak.merzouki@polymtl.ca

Chemical modification of synthetic siRNAs has provided resistance to nuclease degradation and improved blood stability.[18–22] For example, selective addition of a phosphorothioate linkage or substitution with 2′-O-methyl on the C2 position of specific riboses increases nuclease resistance of siRNAs without compromising activity.[14,19,20] Nevertheless, some chemical modifications can increase cytotoxicity, off-target effects and reduce messenger RNA (mRNA) hybridization.[23–27] Despite progress achieved through chemical modification to increase siRNA half-life, transfection efficiency, cellular targeting, and uptake remain as obstacles to effective delivery. Therefore, packaging systems which can both protect and transport chemically unmodified/modified siRNA to target cells are required.

Liposomes/Lipoplexes have been extensively used as nonviral vehicles for plasmid and RNAi entities and pose toxicity concerns. For example, the repeated administration of lipid-based delivery vehicles caused phospholipidosis.[28] Intravenous injection of stable nucleic acid-lipid particles has successfully targeted the liver to silence the *apolipoprotein B* (*ApoB*) gene in mice and nonhuman primates.[10] However, a significant 20-fold transient elevation in serum transaminases (aspartate transaminase, alanine transaminase) indicative of hepatocellular necrosis was identified at the effective dose. Liposomal formulations of nucleic acids are known inducers of inflammatory cytokines including tumor necrosis factor-alpha, interferon-gamma, and interleukin-6 which may be related to liver damage.[29] Polyethylene glycol (PEG) modification of liposomes (PEGylation), for the purpose of reducing their toxicity, was also demonstrated to elicit acute hypersensitivity after repeated dosing.[30–32] Similarly, the highly studied cationic family of polymers such as polyethylenimine demonstrated high gene transfer efficiency but was also associated with significant toxicity issues[1,33] limiting their broad use in clinical trials. Polyethylenimine cytotoxicity was characterized as a two-phase process where the polycation-cell interaction induces loss of cell membrane integrity and the induction of programmed cell death. Insights into polyethylenimine toxicity highlight the importance of polycation/organelle interactions – ie, mitochondria and lysosomes – on the induction of toxicity.[34,35] In general, cationic polymers display less toxicity associated with cytokine induction – immune activation – compared to their cationic lipid counterparts.[36]

Chitosan, a family of cationic polymers of β-1-4 N-acetyl-glucosamine and D-glucosamine residues, has been extensively studied for the delivery of plasmid DNA (pDNA) and siRNA both in vitro and in vivo.[3,8,17,37–43] Chitosan properties include mucoadhesivity,[44] biocompatibility, biodegradability,[45] nontoxicity, and low cost of production. Primary amine residues confer a polycationic nature to chitosan at pH values below its pKa (~6.5) thus enabling it to condense polyanionic compounds such as nucleic acids. Electrostatic interaction between chitosan and nucleic acids leads to the spontaneous formation of nanoparticles of different sizes and shapes.[46] The ability of chitosan-based nanoparticles to transfect cells efficiently depends on several parameters such as: (1) the degree of deacetylation (DDA), which represents the fraction of ionizable monomers; (2) the average molecular weight (M_n), proportional to chain length, and (3) the amine-to-phosphate (N:P) charge ratio represented by the amine-(chitosan)-to-phosphate (DNA or RNA) ratio used to form nanoparticles.

We have previously demonstrated that maximization of in vitro transfection efficiency for the delivery of pDNA depends on a fine balance between these tunable parameters of chitosan[38–40] and found maximum transgene expression for DDA:M_n values that run along a diagonal from high DDA/low M_n to low DDA/high M_n.[38] We have also demonstrated that specific chitosan formulations [DDA, M_n, and N:P ratio] efficiently express transgene in vivo.[37,41]

We also demonstrated that specific formulations are able to trigger an anti-transgene immune response;[37] therefore, nanoparticles can be designed based on the fine-tuning of chitosan parameters for application-specific purposes such as genetic vaccination or gene therapy.

The structural differences between pDNA and siRNA are believed to affect the complexation/stability of nanoparticles and optimal parameters required for effective delivery. Chitosan has also been used for siRNA delivery both in vitro and in vivo.[1,8,10,17,43] However, and despite attempts to identify optimal physicochemical parameters for siRNA delivery,[43] inconclusive results have been observed in the literature due to experimental discrepancies.[8,17] For example, it was reported that intermediate DDA (80%) and high Mw (64–170 kDa) chitosan were more efficient than low molecular weight chitosan (LMW-CS) (10 kDa) in delivering siRNA.[17,43] However, high molecular weight chitosans are found to be cytotoxic,[47–49] thus potentially limiting their use in future clinical trials. Additionally, most of the reports evaluating the physicochemical parameters of chitosan/siRNA nanoparticles were performed at high N:P ratios (N:P >25).[8,17,43] Such formulations bring significant practical problems including limited dosing due to aggregation and the nonspecific effects of large quantities of soluble chitosan.[50] Here, we investigate, for the first time, the ability

of specific LMW-CS formulations (92-10-5, 80-80-10, 80-40-5, and 80-10-10) [DDA, M_n, and N:P ratio] at low N:P ratios to in vitro deliver siRNA targeting: (1) the RecQL1 DNA helicase mRNA in the colon adenocarcinoma RecQL1 overexpressing cell line (LS174T) and (2) ApoB mRNA in the hepatocarcinoma-derived cell line (HepG2). The choice of these two targets resides in their relevance to cancer and atherosclerosis, respectively.[6,7,9,51,52] We also explored the ability of these formulations to transfect multiple cell lines such as A549, AsPC1, HEK293, and Raw264.7 without apparent toxicity. In this study, we hypothesized that, contrary to previous literature,[8,17,42,43] low Mw chitosans (LMW-CS) complexed at low N:P ratios represent suitable formulations for siRNA delivery and gene knockdown; similar to our observations with pDNA.[37–41] Additionally, we hypothesized that low N:P ratios assure sufficient protection and efficient delivery of the siRNA cargo. Moreover, we explore the physicochemical properties of these specific formulations with the prospect of optimizing nanoparticle transfection and silencing efficiencies. Our results demonstrate, for the first time, that LMW-CSs at low N:P ratios are effective and nontoxic delivery systems for polynucleotide and siRNA delivery for in vitro gene silencing.

Materials and methods

Synthesis of siRNAs and dsODNs

siRNAs targeting the RecQL1 DNA helicase and ApoB mRNAs were synthesized using a novel RNA synthesis chemistry, the 5′-silyl-2′-orthoester protecting groups (2′-ACE)[54] combined with a standard phosphoramitide solid-phase technology by Dharmacon (Thermo Scientific, Dharmacon RNAi Technologies, Lafayette, CO). RecQL1 mRNA-specific siRNA (siRNA-RecQL1) contains the sense sequence of 5′-GUUCAGACCACUUCAGCUUdTdT-3′ and antisense 5′-AAGCUGAAGUGGUCUGAACdTdT-3′ whereas ApoB mRNA-specific siRNA (siRNA-ApoB) contains the sense sequence of 5′-GUCAUCACACUGAAUACCAAU-3′ and antisense 5′-AUUGGUAUUCAGUGUGAUGACAC-3′. Mock siRNA was also used as a negative control. Mock siRNA is a nontargeting siRNA (Dharmacon, D-001710-01-05) designed to have minimal targeting of known genes in human, mouse, and rat cells.

Double-stranded oligodeoxynucleotides (dsODNs, 21 bp) encoding the same sequences and mimicking siRNA physicochemical properties were used for nanoparticle characterization. The double-stranded oligodeoxynucleotide (dsODN) sequences were synthesized using the phosphoramidite chemistry (Integrated DNA Technologies Inc, Coralville, IO) and used for size and zeta potential determination, nanoparticle stability, and nuclease protection assays. For confocal microscopy and flow cytometry analysis, 6-carboxyfluorescein (6FAM) 5′-labeled dsODNs were used (Integrated DNA Technologies Inc). The rationale for using dsODN for chitosan nanoparticle physicochemical characterization is their siRNA-mimicking properties. These mimicking properties are due to similarities at the structural level (double-stranded structure, length, and nucleotide overhangs) between siRNA and dsODNs. Additionally, charge densities are similar between siRNA and dsODNs due to identical phosphate residue numbers on their backbone. The main differences between siRNA and dsODNs lie in the substitution of uracil to thymine (U → T) in the dsODN sequences, and in the deoxyribosilation of the dsODN sugar backbone.

Preparation and characterization of depolymerized chitosan

Clinical-grade chitosan at different DDAs was obtained from BioSynthec Inc, (Laval, QC, Canada) and depolymerized using nitrous acid to achieve specific number-average molecular weight targets (M_n) of 80, 40, and 10 kDa. Chitosan number- and weight-average molecular weights (M_n and M_w) were determined by gel permeation chromatography using a Shimadzu LC-20AD isocratic pump, autosampler SIL-20AC HT, oven CTO-20AC coupled with a Dawn HELEOS II multiangle laser light scattering detector (Wyatt Technology Co, Santa Barbara, CA), a Viscostar II (Wyatt Technology Co), an Optilab rEX interferometric refractometer (Wyatt Technology Co), and two Shodex OHpak (SB-806M HQ and SB-805 HQ; Showa Denko America, Inc, New York, NY) columns eluted with a pH 4.5 acetic acid (0.15 M)/sodium acetate (0.1 M)/sodium azide (4 mM) buffer.[54,55] The injection volume was 100 µL, the flow rate 0.8 mL min^{-1} and the temperature 25°C. The dn/dc value was previously calculated for chitosan with a DDA of 92% (for a laser's wavelength of 658 nm) and is equal to 0.208 and 0.201 for chitosan with 80% DDA. The degree of deacetylation was determined by ^{1}H NMR according to our previous reports.[38,56]

Preparation of chitosan nanoparticles

Chitosans with specific M_n and DDA (Table 1) were dissolved overnight on a rotary mixer at 0.5% (w/v) in hydrochloric acid using a glucosamine:HCl ratio of 1:1 at a final concentration of 5 mg/mL. Sterile filtered solutions were then diluted with deionized water to obtain the desired ratio

Table 1 Physicochemical characteristics of bulk chitosans

Chitosan	DDA (%)[a]	M_n (kDa)[b]	M_w (kDa)	PDI[c]	N:P ratio[d]
92-10	92	10	11.8	1.5	5
80-10	80	10	14.5	1.3	10
80-40	80	40	53.0	1.3	5
80-80	80	80	110.9	1.6	5

Notes: [a]As determined by 1H NMR; [b]as determined by gel permeation chromatography (GPC); [c]M_w/M_n; [d]nanopartice N:P ratio follwing complexation with either dsODN or siRNA used in this study.
Abbreviations: DDA, degree of deacetylation; M_n, number average molecular weight; M_w, specific molecular weight; PDI, polydispersity index; N:P, amine to phosphate; dsODN, double-stranded oligodeoxynucleotides.

(N:P) of amine (chitosan deacetylated groups) to phosphate (dsODNs/siRNA nucleic acids). Nanoparticles (92-10-5, 80-10-10, 80-40-5, and 80-80-5) were then prepared by rapid mixing (pipetting) of 100 µL of diluted chitosan solution to 100 µL of dsODNs or siRNA at a concentration of 0.05 µg/µL or 100 nM.

Nanoparticle size and ζ-potential analysis

The size of chitosan/dsODN-RecQL1 and chitosan/dsODN-ApoB nanoparticles – intensity average diameter – was determined by dynamic light scattering at an angle of 173° at room temperature using the Malvern Zetasizer Nano ZS (Malvern, Worcestershire, UK). Following nanoparticle formation, samples were diluted in 10 mM NaCl at a ratio of 1:10 and measured in triplicate. The ζ-potential was measured in triplicate using laser Doppler velocimetry at 25°C on the same instrument with the viscosity and dielectric constant of pure water used for calculations.

Environmental scanning electron microscopy (ESEM)

Chitosan/dsODN-RecQL1 and chitosan/dsODN-ApoB nanoparticles were sprayed on silicon wafer substrate then sputter-coated with gold (Agar Manual Sputter Coater; Marivac Inc, Montreal, QC, Canada) and imaged using a Quanta 200 FEG Environmental Scanning Electron Microscope (FEI Inc, Hillsboro, OR). Observations were performed at 20 kV using the high-vacuum mode. The average particle diameter (± standard deviation) was determined using the XT Docu image analysis software (FEI Inc).

Nanoparticle stability assessment by polyacrylamide gel electrophoresis

The stability of chitosan/dsODN nanoparticles at different pHs (6.5 and 8) and for different incubation times (0.5, 4, and 24 hours) was assessed using polyacrylamide gel electrophoresis. Upon formation, nanoparticles were mixed at a ratio of 1:1 with 2-(N-morpholino)ethanesulfonic acid buffer (MES 1X) (20 mM MES, 8 mM sodium acetate, pH 6.5) or Tris-acetate (TAE)-EDTA buffer (TAE 1X) (2 M Tris-acetate, 50 mM EDTA, pH 8). The samples were then migrated on a 13% polyacrylamide gel (BioRad Laboratories, Mississauga, ON, Canada) for 2 hours at 100 mV in either MES or TAE buffer. Gels were stained with 0.5 µg/mL ethidium bromide solution (BioRad Laboratories) to visualize dsODNs. Gel documentation and image analysis were performed using a Bio-Vision 3000 (Vilbert Lourmat, Marne-la-Vallée, France) and the Vision-Capt software, respectively.

Nuclease protection assay

The level of protection against nuclease attack offered by chitosan formulations (92-10-5, 80-80-10, 80-40-5, and 80-80-5) was assessed electrophoretically on a 5% agarose gel. Chitosan/dsODN-RecQL1 and chitosan/dsODN-ApoB nanoparticles at different DDA, M_w, and N:P ratios were incubated with 0.5, 1, 2, 5, or 10 units of DNAse I (Sigma-Aldrich, Oakville, ON, Canada) per µg of dsODNs in 20 µL of MES-$MgCl_2$ buffer (20 mM MES, 1 mM $MgCl_2$, pH 6.5) for 30 minutes at 37°C. The reaction was stopped by adding 2 µL of EDTA (50 mM) (Sigma-Aldrich). To ensure proper migration of the nondigested dsODNs, samples were treated with *Streptomyces griseus* type III chitosanase (Sigma-Aldrich) at 10 mU/µL for 1.5 hours at 37°C and stopped by placing the samples at –20°C for 15 minutes as previously described.[3] Samples were migrated at 90 V during 1 hour then stained with 0.5 µg/mL ethidium bromide solution before visualization. Captured images were analyzed using Vision-Capt software (v 15.06; Vilber Lourmat, Paris, France). Relative amounts of dsODN-RecQL1 or dsODN-ApoB (%) were determined by comparison of the integrated signal intensity of nuclease-treated samples versus nontreated samples.

In vitro cell transfection

Cell culture

All cell lines were purchased from American Type Cell Culture (Manassas, VA). The HepG2 cell line was cultured in minimal essential medium (MEM). The HEK293, Raw294.7, and LS174T cell lines were cultured in high-glucose Dulbecco's modified eagle's media (DMEM-HG). The A549 and AsPC1 cell lines were cultured in F12-K and Roswell Park Memorial Institute medium media, respectively. All cell culture media contained 1.85 g/L of sodium bicarbonate ($NaHCO_3$) and were supplemented with 10% fetal bovine serum (Cedarlane Laboratories, Burlington, ON, Canada).

All cell lines were cultured at 37°C in a 5% CO_2 incubator. For transfection, cells were plated in 96-well or 24-well culture plates (Corning, Lowell, MA) to obtain a ~50% confluence the day of transfection using 100 µL/well or 500 µL/well, respectively, of complete culture medium.

Cell transfection

For in vitro transfection, DMEM-HG was prepared with 0.976 g/L of MES and 0.84 g/L of $NaHCO_3$ at a pH of 6.5. Transfection media containing 10% fetal bovine serum was equilibrated overnight at 37°C in a 5% CO_2 incubator and the pH was adjusted to 6.5 using sterile HCl (1N) prior to transfection. For siRNA transfection performed in a 96-well plate, chitosan/siRNA nanoparticles were prepared as described above, 30 minutes before use. A 100 µL siRNA solution at a concentration of 0.05 µg/µL was used for siRNA complexation with chitosan at a 1:1 ratio (v/v). Following complexation, nanoparticles were incubated in a ghost plate containing the transfection media (DMEM-HG + fetal bovine serum) at a final concentration of 1.35 ng/µL; equivalent to 10 pmol per well of siRNA. For dsODN transfection performed in a 24-well plate, nanoparticles were complexed as described above and incubated at a final concentration of 8.07 ng/µL, equivalent to 60 pmol per well of dsODNs. Plates containing nanoparticles were equilibrated for 10 minutes at 37°C, 5% CO_2. Medium over cells was aspirated and replenished with either 500 µL (24-well plate) or 100 µL per well (96-well plate) of the transfection medium containing dsODN- or siRNA-based nanoparticles. Cells were incubated with chitosan/siRNA or chitosan/dsODN nanoparticles until analysis 24 hours post transfection. The commercially available liposome, DharmaFECT™ (Dharmacon RNAi Technologies), was used as a positive control and both untreated cells and uncomplexed siRNA/dsODN-treated cells were used as negative controls.

Transfection with DharmaFECT

DharmaFECT was used as a positive control for transfection efficiency in all tested cell lines. DharmaFECT/dsODN (flow cytometry and confocal microscopy) or DharmaFECT/siRNA (qPCR and viability assay) lipoplexes (1:2 [w/v] ratio) were prepared following the manufacturer's protocol.

In vitro cell viability assay

Nanoparticle toxicity was evaluated using the alamarBlue® proliferation assay (Invitrogen, Carlsbad, CA). The principle of the assay is based on the natural reducing power of viable cells to convert resazurin, a blue and nonfluorescent compound, into resofurin; a red and fluorescent molecule. Viable cells continuously convert resazurin to resofurin, thereby providing a quantitative measure of viability. Transfection was performed as described above using chitosan-siRNA nanoparticles. Five thousand cells/well were seeded 24 hours before transfection. To alleviate the experimental bias from the effect of RecQL1 gene silencing on cell viability, nontargeting siRNA (siRNA mock) was used instead. Twenty-four hours post transfection with chitosan-based nanoparticles, 20 µL of alamarBlue reagent, pre-warmed at 37°C was added to each well and incubated for another 4 hours. At the end of the incubation 100 µL of media containing reduced alamarBlue dye was transferred to a black Corning 96-well plate and read on an infinite 200 fluorescence plate reader (Tecan Systems, San Jose, CA) with excitation 560 nm, emission 590 nm and a cut-off of 570 nm. Cells without the addition of alamarBlue were used as blank and dimethyl sulfoxide was used as a positive control of toxicity. The viability of nontransfected control cells was arbitrarily defined as 100%. The relative cell viability was calculated using the following formula: (fluorescence $\text{intensity}_{\text{sample}}$/$\text{fluorescence intensity}_{\text{control}}$) × 100.

Uptake analysis by flow cytometry and confocal microscopy

Fluorescence-activated cell sorting (FACS) analysis

The cellular uptake of dsODNs was determined by transfecting AsPC1, A549, LS174T, HepG2, HEK293, and Raw264.7 cell lines with nanoparticles formed with (6FAM) 5′labeled dsODNs. Twenty-four hours post-transfection, cells were chitosanase treated for 60 minutes to eliminate any cell surface-associated nanoparticles left from the transfection as described previously.[3] Afterward, cells were washed twice with phosphate-buffered saline, trypsinized, and resuspended in phosphate-buffered saline. The analysis of cell uptake was made using a BD Canto flow cytometer (Becton Dickinson, San Jose, CA). For each sample, 20,000 events were counted and to exclude cell debris, dead cells, and aggregated cells, a collection gate was established using a dot plot of the forward light scatter against the side scatter. Nontransfected cells were used as negative controls to discriminate (6FAM) positive cells from auto-fluorescence.

Confocal microscopy

For nanoparticle internalization analysis, the LS174T, HepG2, HEK293, and Raw264.7 cell lines were seeded on 35 mm glass-bottom culture dishes (MatTek, Ashland, MA) at 40,000 cells/dish using 500 µL of complete culture medium.

Nanoparticles were formed with fluorescent rhodamine B isothiocyanate-labeled chitosan and dsODNs labeled with 6FAM on their 5′ extremities (Integrated DNA Technologies). Prior to imaging, cell membranes were stained with 5 μg/mL of Cell Mask™ Deep Red (Invitrogen, Burlington, ON, Canada). Images were taken in multitrack mode using a Zeiss LSM 510 META confocal Axioplan 200 microscope (Carl Zeiss AG, Feldbach, Switzerland). Chitosan and dsODNs were visualized as red and green pseudocolors, respectively. The spatial overlap of these two colors produced yellow which permitted a qualitative assessment of colocalization.

Quantitative PCR (qPCR) analysis of RecQL1 and ApoB mRNA knockdown

RNA extraction and assessment methods (yield, purity, and integrity)

RNA extraction was performed using the RNA XS® extraction kit from Macherey-Nagel (Biolynx, Montréal, QC, Canada) according to the manufacturer's protocol following chitosanase treatment, as described previously.[3] Total RNA was quantified and RNA integrity was measured using the Agilent BioAnalyzer 2100 (Agilent Technologies, Mississauga, ON, Canada) following the manufacturer's protocol. RNA integrity was evaluated by the ratio of 28S/18S ribosomal RNA[57] and the RNA integrity number (RIN). The Agilent 2100 BioAnalyzer uses automated microfluidics, capillary electrophoresis, and fluorescence to evaluate RNA integrity. The RIN is a relative measure of RNA quality that is based largely on electrophoretic trace analysis. The BioAnalyzer 2100 automatically computes RIN, where an ideal nondegraded RNA sample has RIN = 10.

Reverse transcription

Total RNA was reverse transcribed in a final volume of 20 μL using the First Strand cDNA Transcriptor Kit (Roche Diagnostics, Laval, QC, Canada) with oligodT primers as described by the manufacturer's protocol. Samples were stored at –20°C.

Gene expression assays

The RecQL1 and ApoB mRNA expression level was determined using assays designed with the Universal Probe Library (UPL) from Roche (Roche Applied Science, Laval, QC, Canada). Endogenous control (hypoxanthine guanine phosphoribosyl transferase) and glyceraldehyde 3-phosphate dehydrogenase expression levels were determined using pre-validated TaqMan® Gene Expression Assays (Applied Biosystems, Carlsbad, CA). RecQL1 and ApoB mRNA (target detection) reactions for 384-well plate formats were performed using 1.5 μL of cDNA samples (25–50 ng), 5 μL of the Fast Universal qPCR MasterMix (Applied Biosystems) 2 μM of each primer, and 1 μM of a Universal Probe Library probe (RecQL1 [probe #29]/ApoB [probe #55]) in a total volume of 10 μL. For endogenous control assessment, reactions were performed using identical volumes of cDNA and, Fast Universal qPCR Master Mix, 0.5 μL of the TaqMan Gene Expression Assay (20×) and 2.5 μL of water in a total volume of 10 μL.

Detection and analysis

The ABI PRISM® 7900HT Sequence Detection System (Applied Biosystems) was used to detect the amplification level and was programmed with an initial step of 3 minutes at 95°C, followed by 45 cycles of 5 seconds at 95°C and 30 seconds at 60°C. All reactions were run in triplicate and the average values of Cts (threshold cycle) were used for quantification. Glyceraldehyde 3-phosphate dehydrogenase and hypoxanthine guanine phosphoribosyl transferase were used as endogenous controls. The relative quantification of target genes was determined using the ρρCT method. Briefly, the Ct values of target genes were normalized to an endogenous control gene (endogenous control) ($\Delta CT = Ct_{target} - Ct_{endoC}$) and compared with a calibrator: $\Delta\Delta CT = \Delta Ct_{target} - \Delta Ct_{calibrator}$. Relative expression (RQ) was calculated using the Sequence Detection System 2.2.2 software using the $RQ = 2^{-\Delta\Delta CT}$ formula.

Statistical analysis

The statistical analysis was performed using Statistica 9.0 Software (STATSOFT; Statistica, Tulsa, OK). Data are expressed as mean ± standard deviation. Statistical significance was determined with one-way analysis of variance, followed by Tukey's post hoc test. The results were considered significant and highly significant ($P < 0.05$ and $P < 0.01$, respectively).

Results

Size and ζ-potential of chitosan nanoparticles

All formulations of chitosan/dsODN nanoparticles were in the range of 41–109 nm as measured by environmental scanning electron microscopy (ESEM) and dynamic light scattering (Figure 1 and Table 2). Chitosan/dsODN nanoparticles showed higher size values with increasing M_n. No statistically significant differences were observed when comparing DDAs

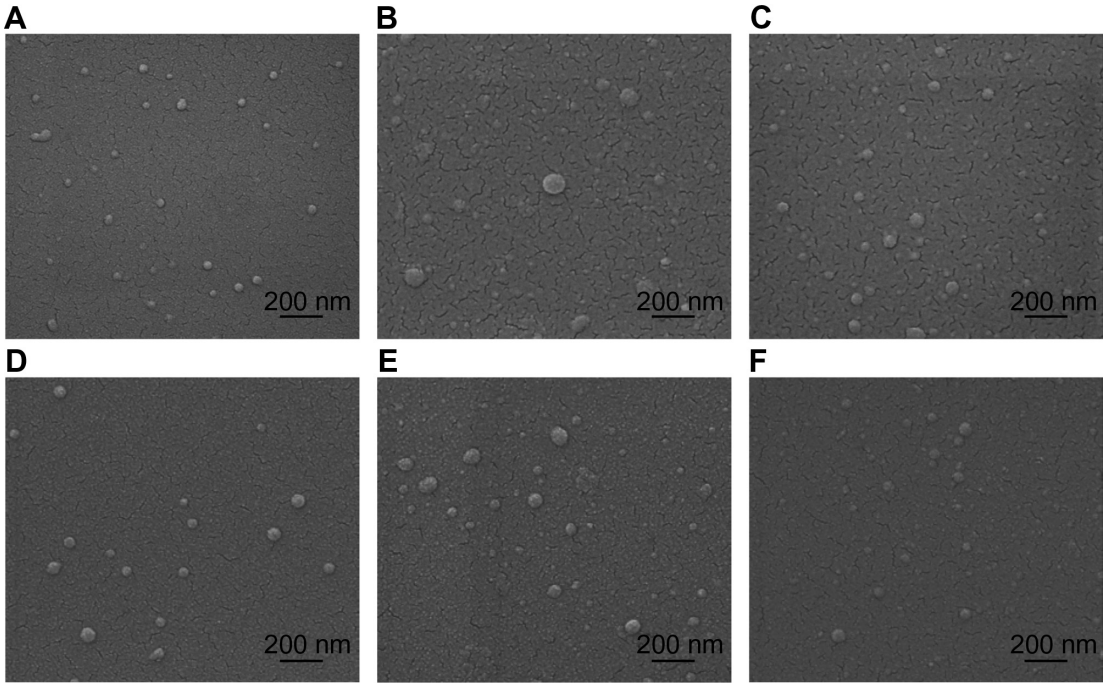

Figure 1 Environmental scanning electron microscopy images of spherical chitosan/dsODN nanoparticles. (**A**) 92-10-5 chitosan/dsODN-RecQL1 nanoparticles; (**B**) 80-40-5 chitosan/dsODN-RecQL1 nanoparticles; (**C**) 80-10-10 chitosan/dsODN-RecQL1 nanoparticles; (**D**) 92-10-5 chitosan/dsODN-ApoB nanoparticles; (**E**) 80-80-5 chitosan/dsODN-ApoB nanoparticles, and (**F**) 80-10-10 chitosan/dsODN-ApoB nanoparticles.
Abbreviations: ApoB, apolipoprotein B; dsODN, double-stranded oligodeoxynucleotide.

for these specific formulations. The excess chitosan in all formulations resulted in positively charged nanoparticles as shown by ζ-potential measurements (Table 2).

Chitosan/dsODN nanoparticle stability

Chitosan-based nanoparticles were incubated for 0.5, 4, and 20 hours in two different buffers (pH 6.5 and 8) to assess the effect of time and pH on nanoparticle stability (Figure 2). Nanoparticles were stable up to 20 hours at an N:P ratio above 2 in slightly acidic buffers (pH 6.5). At 4 hours following nanoparticle formation, and under slightly acidic conditions, no detectable dsODNs were observed at N:P ratios of 2 or higher (Figure 2A and C). On the contrary, dsODN release was observed for the same N:P ratios at a pH of 8 (Figure 2B and D). Longer exposure time – 20 hours – at a pH of 6.5 resulted in increased dsODN-ApoB release at an N:P ratio of 2. This pattern was not observed for the dsODN-RecQL1 sequence. This may be due to sequence/structural differences between the two dsODNs. Furthermore, our results at a pH of 8 show a rapid partial-to-complete dsODN release after 0.5 hour at an N:P ratio of 2 (Figure 2B and D). At N:P ratio 10 and for the same pH of 8, chitosan showed a partial release of dsODNs indicating the effect of excess chitosan on preserving stability. Overall, our specific chitosan formulations assured nanoparticle stability for a minimum period of 20 hours at an N:P ratio above 2 in slightly acidic near-neutral pH environments.

Table 2 Size and zeta potential values obtained by dynamic light scattering for chitosan/dsODN-RecQL1 and chitosan/dsODN-ApoB nanoparticles

ODN	Chitosan	Size DLS (nm)	Size ESEM (nm)	Zeta potential (mV)
RecQL1	92-10-5	63 ± 8	54 ± 6	23 ± 1
RecQL1	80-40-5	86 ± 9	97 ± 12	18 ± 1
RecQL1	80-10-10	91 ± 7	73 ± 9	18 ± 2
ApoB	92-10-5	45 ± 4	66 ± 5	21 ± 2
ApoB	80-80-5	100 ± 8	75 ± 13	16 ± 1
ApoB	80-10-10	64 ± 6	67 ± 7	19 ± 2

Notes: Values are mean ± SD; n = 3.
Abbreviations: ApoB, apolipoprotein B; dsODN, double-stranded oligodeoxynucleotides; DLS, dynamic light scattering; ESEM, environmental scanning electron microscopy; SD, standard deviation.

Nanoparticle protection assay

For effective gene expression and/or inhibition, nucleic acids entrapped in the delivery vehicle must be protected from degradation by enzymes such as serum nucleases.[58] The ability of chitosan-based nanoparticles to protect siRNA mimicking dsODN sequences was assessed using a DNAse I protection assay against different chitosan formulations complexed with dsODN-RecQL1 or dsODN-ApoB. Upon incubation

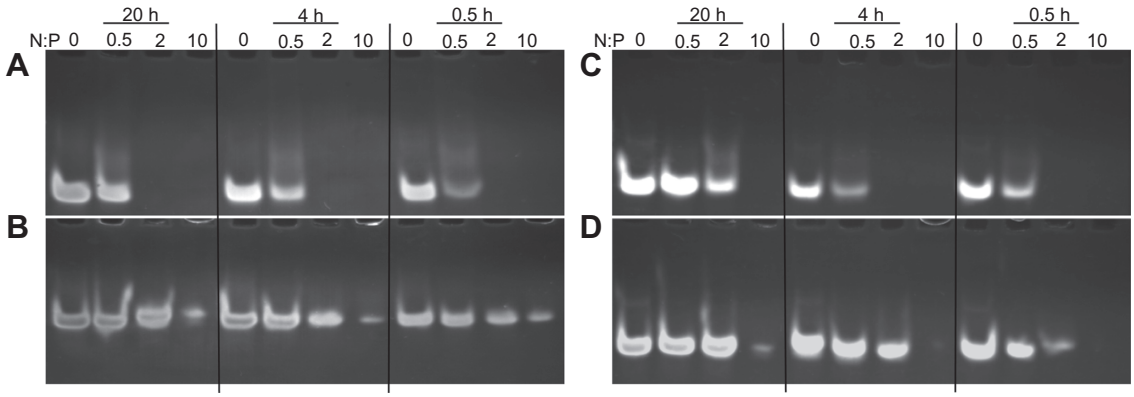

Figure 2 Chitosan nanoparticle temporal stability. Stability was assessed at 0.5, 4, and 24 hours after complex formation using polyacrylamide gel electrophoresis at a pH of 6.5 (MES 1X) and pH8 (TAE 1X). Chitosan 92-10 at different N:P ratios (0.5, 2, and 10) was complexed with: (**A**) dsODN-RecQL1 at a pH of 6.5; (**B**) dsODN-RecQL1 at a pH of 8; (**C**) dsODN-ApoB at a pH of 6.5, and (**D**) dsODN-ApoB at a pH of 8. Unstable nanoparticles release dsODNs which become visible following EtBr staining on polyacrylamide gel following ethidium bromide staining of the polyacrylamide gel.
Abbreviations: ApoB, apolipoprotein B; dsODN, double-stranded oligodeoxynucleotide; N:P, amine to phosphate.

with DNAse I, naked dsODN-RecQL1 and dsODN-ApoB (controls) were completely degraded (Figure 3A–D, lane 3). In contrast, DNAse I protection assay showed that all chitosans tested protected dsODNs from degradation at DNAse I concentrations <2 units DNAse I per µg dsODN (Figure 3). Chitosan formulations demonstrated an average of ~80% protection of dsODNs at DNAse I concentrations of 0.5 U/µg (Figure 3). The ability of LMW-CS (92-10, 80-40, 80-80, and 80-10) to protect dsODNs from nuclease degradation decreased with increased concentrations of DNAse I. Our results show that protection decreased from ~50% at a DNAse I concentration of 1 U/µg to less than ~20% at 2 U/µg (92-10 and 80-10). Moreover, our results suggest that higher M_n chitosan (80-40 and 80-80) offers a slightly better protection of dsODNs as compared to lower M_n chitosan (92-10 and 80-10) at high DNAse I concentrations (2 U/µg) (Figure 3A–D). The enhanced cargo protection observed with higher molecular weight chitosans is consistent with previous studies where higher binding affinities between high Mw chitosans and nucleic acids was demonstrated.[59] Altogether, our results show that DNAse I protection is considerable when using intermediate to low DDA/M_n and preserves approximately 60% of nucleic acid when using 1 unit of DNAse I per µg of dsODNs.

In vitro cell uptake analysis by flow cytometry and confocal microscopy

Nanoparticle internalization into cells can be another rate-limiting step for effective drug delivery systems. In general, efficient nanoparticle internalization depends on several factors, such as the cell type, the physicochemical surface properties of the nanoparticles, and the bio–nano interface.[60] The internalization of RecQL1- and ApoB-bearing nanoparticles was assessed in two different sets of relevant cell lines using flow cytometry (FACS). For the assessment of (6FAM) dsODN-RecQL uptake, transfection and FACS analysis were performed on AsPC1, A549, and LS174T cancer cell lines whereas (6FAM) dsODN-ApoB uptake was performed on HEK293, HepG2, and Raw269.7 cell lines. Our FACS results show that cell uptake using chitosan/(6FAM) dsODN-ApoB nanoparticles achieved levels comparable to the commercially used lipoplex (DharmaFECT) (Figures 4 and 5), demonstrating the internalization efficiency of LMW-CS formulations in different cell lines. Moreover, our results indicate that different chitosan formulations show statistically significant differences in their cell uptake efficiency, with LMW-CSs 92-10-5 and 80-10-10 more easily internalized compared to the higher molecular weight 80-80-5 and 80-40-5, in a cell-line-dependent manner. Interestingly, the A549 and HEK293 cell lines demonstrated no statistical differences in uptake efficiency between the different chitosan formulations (Figures 4 and 5A). However, the A549 and HEK293 cell lines showed statistically significant increases in uptake when compared to the LS174T and Raw264.7 cell lines, again highlighting some important cell-type dependencies.

In general, LMW-CS (92-10-5 and 80-10-10) showed higher uptake efficiency, ranging from approximately 65% to 95% depending on the transfected cell line (Figures 4 and 5A). These results are in accordance with confocal microscopy data, where images representative of the whole population show that the vast majority of cells for each of the four cell types imaged show nanoparticle internalization (Figure 6). The lack of colocalization at 24 hours between dsODNs and chitosan indicates that complete release of the dsODN cargo

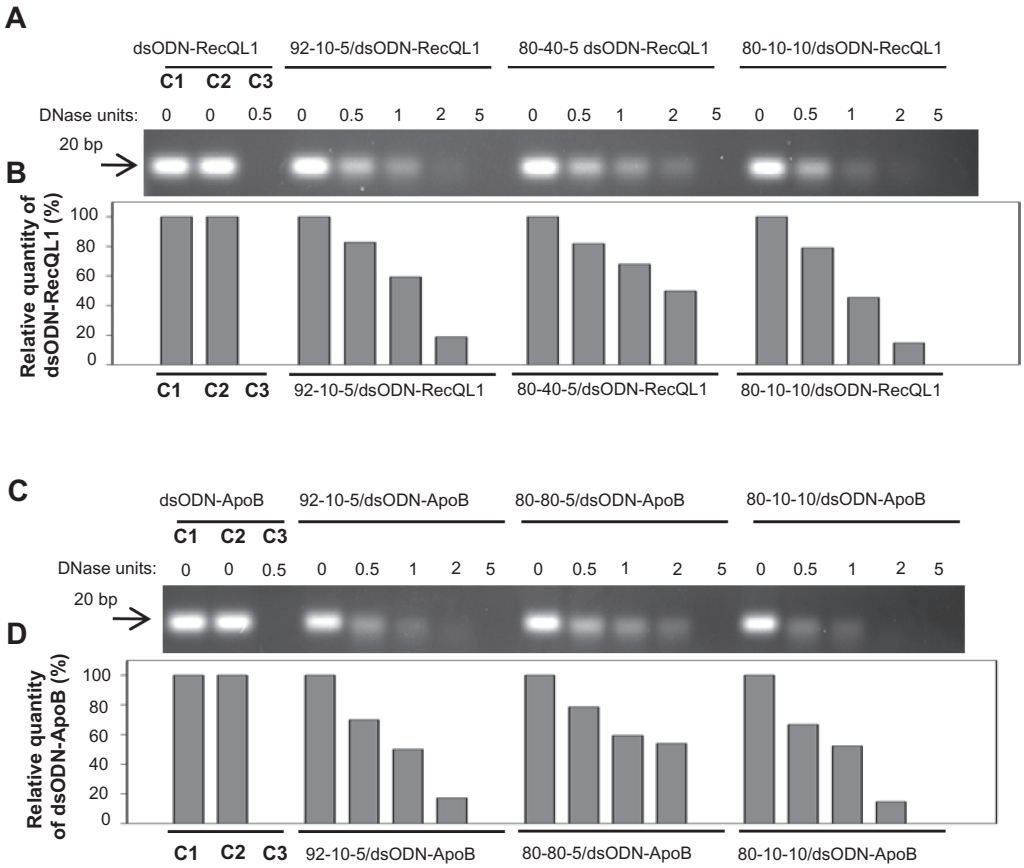

Figure 3 Nuclease protection assays of chitosan/dsODN nanocomplexes. (**A**) Chitosan (92-10-5, 80-40-5 or 80-10-10) complexed with dsODN-RecQL1. (**B**) dsODN-RecQL1 remaining after the DNAse I digestion was assessed using the signal intensity of the treated samples with the control (ie, 0 U DNAse I = 100% intensity). This comparison was made between the samples of the same chitosan formulation. (**C**) Chitosans (92-10-5, 80-80-5 or 80-10-10) complexed with dsODN-ApoB. (**D**) dsODN-ApoB remaining after the DNAse I digestion was similarly assessed as in (**B**).

Abbreviations: ApoB, apolipoprotein B; dsODN, double-stranded oligodeoxynucleotide.

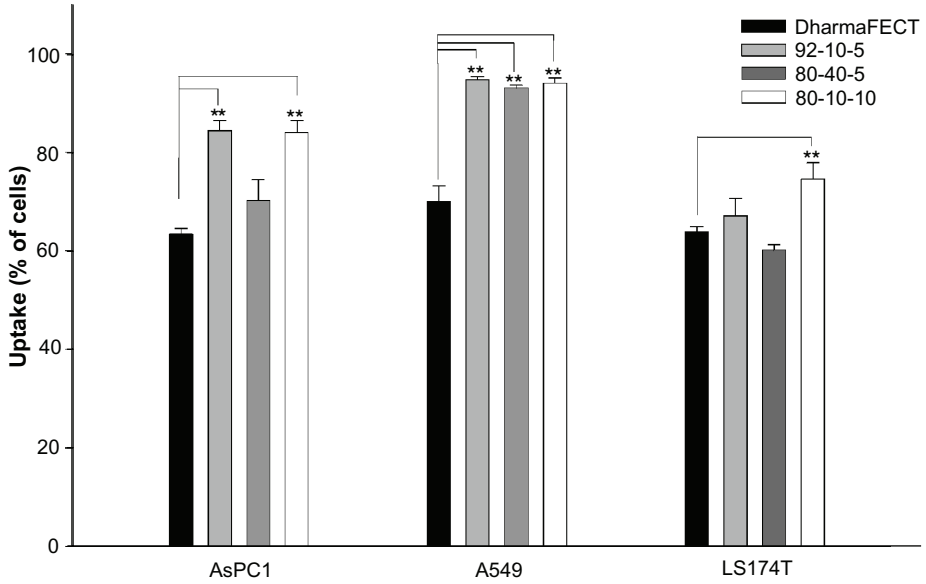

Figure 4 Cellular uptake of dsODN-RecQL1 nanoparticles 24 hours post transfection in AspC1, A549, and LS174T cancer cell lines. Chitosan formulations 92-10-5, 80-40-5, and 80-10-10 were complexed to (6FAM) 5′ labeled dsODN-RecQL1 and transfected at 60 pmol/well 24 hours prior to fluorescence-activated cell sorting analysis. DharmaFECT™ was used as the positive uptake control.

Notes: Values are mean ± SD; n = 3; $^{**}P > 0.01$.

Abbreviations: dsODN, double-stranded oligodeoxynucleotide; SD, standard deviation.

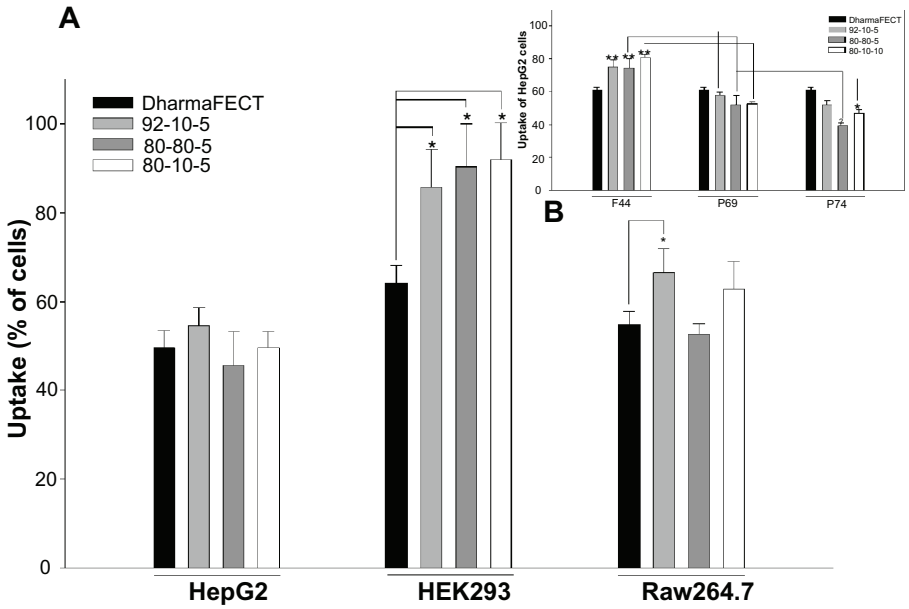

Figure 5 Cellular uptake of dsODN-ApoB nanoparticles 24 hours post transfection in HEK293, Raw269.7, and HepG2 cell lines. Chitosan formulations 92-10-5, 80-80-5, and 80-10-10 were complexed to (6FAM) 5′ labeled dsODN-ApoB and transfected at 60 pmol/well 24 hours prior to fluorescence-activated cell sorting analysis. (**A**) Uptake efficiency of dsODN-ApoB in percentage (%). (**B**) Uptake efficiency of dsODN-ApoB in HepG2 cells at different passage numbers. DharmaFECT™ was used as the positive uptake control.

Notes: Values are mean ± SD; n = 3; *$P > 0.05$; **$P > 0.01$.

Abbreviations: ApoB, apolipoprotein B; dsODN, double-stranded oligodeoxynucleotide; SD, standard deviation.

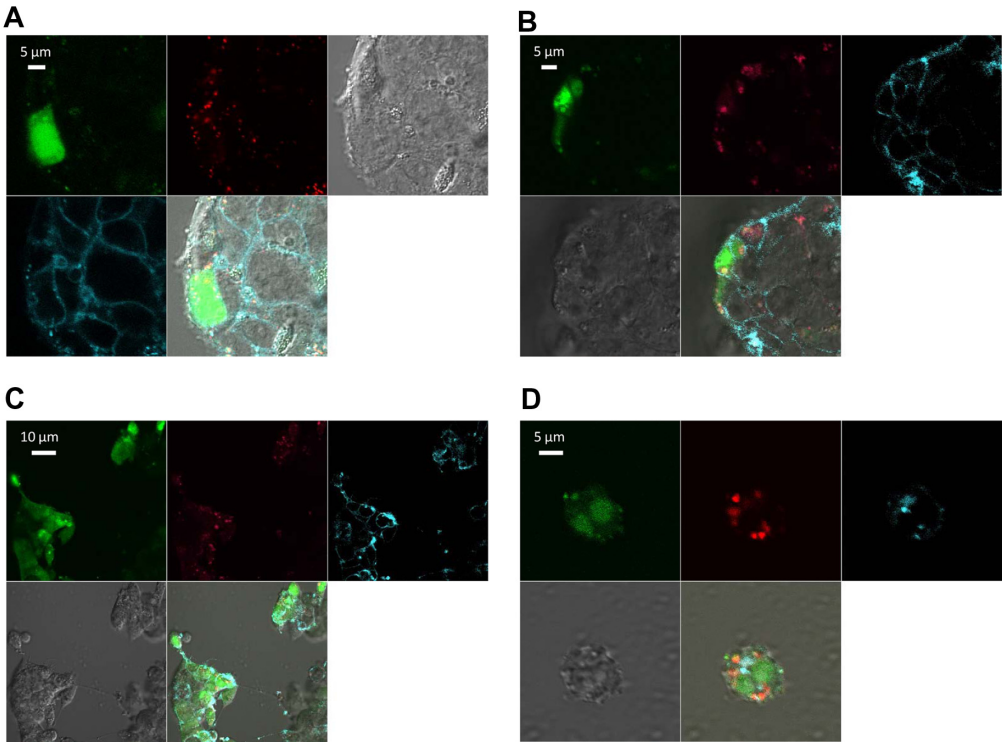

Figure 6 Confocal imaging of chitosan/dsODN nanocomplex uptake 24 hours post transfection. Chitosan 92-10 (DDA, M_n) was labeled with rhodamine (red) and dsODNs were 5′ labeled with (6FAM) (green). Chitosan 92-10 was complexed to dsODNs at an N:P ratio of 5. Cell membranes were stained prior to imaging with CellMask™ (blue) to differentiate between internalized and membrane-bound nanoparticles. Images shown represent each separate channel, with dsODNs in green, chitosan in red, membrane in blue, differential interference contrast image in grey, and the merged images shown on the bottom left quadrant. (**A**) LS174T cells transfected with chitosan/dsODN-RecQL1 nanoparticles. (**B**) HepG2 cells transfected with chitosan/dsODN-ApoB nanoparticles. (**C**) HEK293 cells transfected with chitosan/dsODN-ApoB nanoparticles. (**D**) Raw 294.7 cells transfected with chitosan/dsODN-ApoB nanoparticles.

Abbreviations: ApoB, apolipoprotein B; dsODN, double-stranded oligodeoxynucleotide; N:P, amine to phosphate.

was achieved 24 hours post transfection. Furthermore, the diffuse staining pattern of dsODNs seen in most transfected cells suggests that complexes have escaped endocytic vesicles (Figure 6), consistent with previous live cell imaging work using chitosan–plasmid DNA nanoparticles.[40]

Specific gene silencing and cell cytotoxicity evaluation of chitosan nanoparticles in different cell lines

Gene silencing occurs when complementarity is achieved between the siRNA seed region and target mRNA.[1] Chitosan-specific formulations (92-10-5, 80-40-5, 80-10-10, and 80-80-5) were assessed for mRNA knockdown in two different cell lines relevant to cancer and atherosclerosis, targeted by RecQL1 and ApoB siRNA, respectively. qPCR analysis revealed inhibition of *RecQL1* and *ApoB* since their coding mRNAs were downregulated more than twofold (Figure 7). More specifically, in LS174T cells, chitosan 92-10-5 showed a high level of silencing (~80%) of RecQL1, similar to the current commercial gold standard liposomal formulation (~80%), used here as a positive control. Formulations 80-40-5 and 80-10-10 also induced significant silencing but to a lower degree than 92-10-5 and also with an increase of nonspecific mock silencing, especially for formulation 80-10-10, for reasons that remain to be elucidated. For the HepG2 cell line, only the best performing 92-10-5 was tested and induced significant silencing (~55% versus ~80% for positive control) of *ApoB* but slightly lower than *RecQL1* for LS174T. Importantly, our results showed that silencing efficiency with chitosan reached similar levels to the positive control, with a markedly reduced cytotoxicity from the delivery system as assessed using the alamarBlue assay (Figure 8).

Discussion

In this study, we evaluated the efficiency of specific low molecular weight chitosan (LMW-CS) formulations at low N:P ratios for the in vitro delivery of siRNA targeting either *RecQL1* or *ApoB* genes. RecQL1 is a DNA helicase playing a major role in homologous recombination, maintenance of genomic stability, and DNA repair at damaged replication forks.[52,61] Overexpression of RecQL1 has been implicated in cancer by preventing cell apoptosis.[6,7,62] As for *ApoB*, it is a major gene involved in atherosclerosis through its essential role in the formation of very low density lipoprotein which will therefore generate low density lipoproteins following triacylglycerol hydrolyzation in the circulation.[51,63,64]

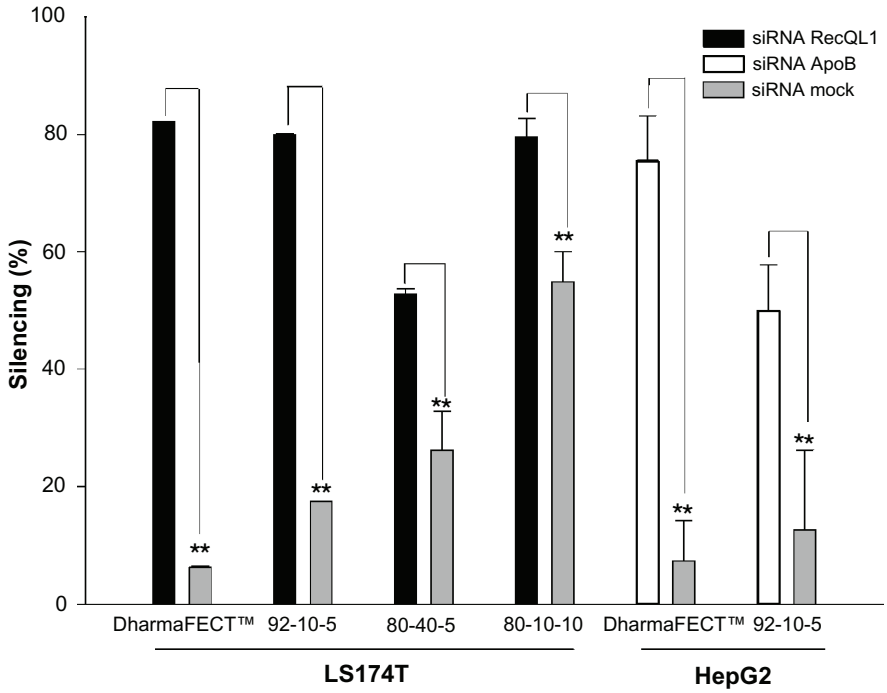

Figure 7 Real-time polymerase chain reaction analysis of the inhibition of RecQL1 and *ApoB* gene expression in specific cell lines. LS174T cells were transfected with chitosan (92-10-5, 80-40-5, and 80-10-10)/siRNA-RecQL1 nanoparticles, whereas HepG2 cells were transfected with chitosan (92-10-5)/siRNA-ApoB nanoparticles. The inhibition percentage was obtained by comparing the transfected and nontransfected cells, using the ΔΔCT method.
Notes: Values are mean ± SD; n = 3; $^{**}P > 0.01$.
Abbreviations: ApoB, apolipoprotein B; siRNA, small interfering RNA; SD, standard deviation.

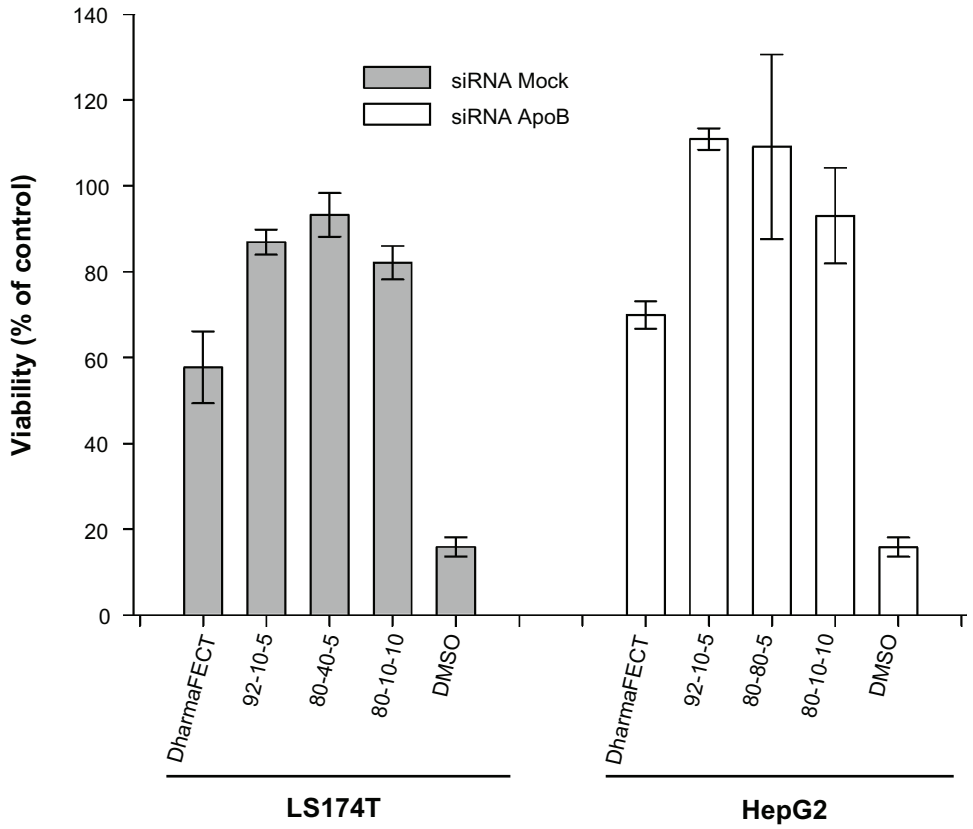

Figure 8 Cell viability assessment using the alamarBlue® assay 24 hours post transfection with different chitosan/siRNA formulations. To alleviate the apoptotic effect of RecQL1 gene silencing for a proper assessment of chitosan-siRNA toxicity, mock siRNA was used for transfection in the LS174T cell line. The HepG2 cell line was transfected with ApoB siRNA. DharmaFECT™ was used for comparison purposes whereas dimethyl sulfoxide was used as a positive control of toxicity.
Notes: Values are presented as mean ± SD; n = 3.
Abbreviations: ApoB, apolipoprotein B; siRNA, small interfering RNA.

Nanoparticle size is one parameter affecting uptake and intracellular trafficking, both considered as potential rate-limiting steps for effective gene therapy.[41,42] For instance, nano-sized particles have been shown to be internalized more efficiently than micro-sized particles.[65–67] In this study, LMW-CS-based nanoparticles ranged in size from 41–110 nm, a size range promoting uptake, prolonged blood circulation, higher tissue penetration, and a relatively free passage from the mononuclear phagocyte system.[48,68–70] Therefore, our results show that these specific LMW-CS nanoparticles at low N:P ratios meet performance criteria (Table 3) and are potentially relevant for in vivo administration. The different chitosan parameters – DDA, M_n, and N:P ratios – used in this study did not significantly affect nanoparticle size, with higher molecular weight chitosan promoting a slightly increased size (Table 1). Our results are in contrast to previously published reports where the authors found increased nanoparticle size for lower molecular weight chitosan.[43] This discrepancy may be due to differences in experimental conditions and to the high N:P ratio used in Liu et al and Howard et al reports[8,43] versus low N:P ratios reported in our study. ESEM analysis revealed that these small nanoparticles were of spherical shape consistent with previous findings for pDNA,[37] siRNA,[8] and dsODNs.[71] The effect of nanoparticle shape on internalization efficiency showed spherical particles of similar size being internalized 500% more efficiently than rod-shaped particles.[72–74] This is mainly explained by increased membrane-wrapping time required for elongated particles and greater thermodynamic forces required for their engulfment.[60,74] It was previously demonstrated that the morphology of chitosan-pDNA nanoparticles is strongly dependent upon their charge ratios, and the variation of the latter resulted in nanoparticles with different topological conformations including spherical,[75] toroidal,[76,77] and globular morphologies.[76,78] Chitosan-based nanoparticle shape may also seem to be affected by the type of nucleic acid – pDNA or siRNA/dsODN – used for complexation and the process of nanoparticle formation; ie, ionic gelation. The fact that these LMW-CS nanoparticles demonstrated a reproducible pattern of spherical particles at low N:P ratios may be indicative of higher internalization efficiency than nanoparticles of different topological conformations.

Table 3 Safety and performance criteria for the development of effective nonviral gene delivery systems

Categories	Performance criteria**
Physical and chemical properties	• Nanoparticle formation/assembly at a nucleic acid scale of 10 mg, from the perspective of size, shape, aggregation, and charge, as well as from an efficacy standpoint (such as toxicity and transfection efficacy), should be similar/reproducible each time nanoparticles are formed at this and lower concentrations • Assemblies less than 300 nm, PDI (<0.3) and no less than 80% incorporation efficiency • No aggregation in 50% mouse/human serum • Chemical stability of the assembly for >30 days • Preferably amenable to freeze-drying without any loss of its performance criteria
Activity in cell based assays*	• >50% reducation in target mRNA by target specific siRNA at concentrations <100 nm in 10% serum containing media • <10% reduction in target mRNA by control siRNA at concentrations <100 nm in 10% serum containing media • >5-fold window between target gene silencing IC50 and IC50 for reduction in viability • Activity in at least relevant 3 cell lines to the delivery system under evaluation
Performance and safety in animal models	• >50% reduction in target mRNA levels by target siRNA and <10% reduction in target mRNA levels in target tissue at 1 mg/kg dose by control siRNA by 24–48 hr • Demonstration of RNAi-mediated target mRNA cleavage by 5'-RACE • <10-fold cytokine induction (TNFα, IFNβ, IL6) and <10-fold increase in ALT and AST at 3 mg/kg siRNA dose • No effect on body weight and normal blood clinical chemistry and hematology data • Lack of immunogenicity • Lack of auto-antibodies and anti-DNA antibodies • Lack of systemic toxicity • No effect on body weight and normal blood clinical chemistry and hematology data

Notes: *If the delivery platform incorporates a targeting moiety evidence should be provided for targeting by (a) using cell lines with differential expression of targeted receptor and (b) using assemblies with "active" and "inactive or mutant" targeting moieties; **performance criteria described here are for both siRNA and plasmid DNA delivery systems. The criteria in this table has been adapted from information in US FDA[84,85] and US Pharmacopeia.[86]

Abbreviations: PDI, polydispersity index; mRNA, messenger RNA; siRNA, small interfering RNA; IC50, half maximal inhibitory concentration; RACE, rapid amplification of cDNA ends; ALT, alanine transaminase; AST, aspartate transaminase.

Nanoparticle stability and nucleic acid protection are important parameters for efficient nucleic acid delivery. Our results of nuclease protection indicate that all LMW-CS formulations tested were able to protect dsODNs at supraphysiological concentrations of nucleases. Nuclease protection is of great importance for nucleic acid delivery systems through maintenance of cargo bioavailability and improved pharmacokinetic profile, thereby increasing the therapeutic potential of these nanoparticles. Increasing chitosan molecular weight resulted in an enhanced cargo protection (Figure 3) in agreement with previous findings.[17,38,42,43,46] Nevertheless, enhancing the ability of nanoparticles to protect their siRNA from degradation may render their intracellular disassembly more difficult, as demonstrated with high molecular weight chitosan-pDNA nanoparticles.[40] Further characterization of nanoparticle stability by gel retardation assays show that LMW-CS used at low N:P ratios can effectively complex and compact dsODNs into stable particles. We found LMW-CS nanoparticles at N:P ratios above 2 to be stable in slightly acidic buffers for at least 20 hours. These interesting findings are in contrast with most previous studies using chitosan-siRNA nanoparticles, where high M_n and high N:P ratios are usually required to achieve particle stability.[8,17,42,43,79] This discrepancy can be explained by the lower pH (pH 6.5) of the electrophoresis buffer in our study compared to the commonly used TAE buffer at a pH of 8 for chitosan-based nanoparticle characterization,[8,17,42,43,80] a difference that was clearly highlighted by our gel retardation assay performed at both pHs (Figure 2). The use of a lower pH in the electrophoresis buffer results in higher degrees of chitosan ionization which translates to stronger electrostatic attraction to the polyanionic nucleic acid and hence more stable nanoparticles. This simple modification of the pH permits lower N:P ratios than those observed previously[8,17,42,43,80] to achieve nanoparticle stability. A direct consequence of this modification translates into reduced dosing, aggregation, and other undesirable nonspecific effects of large quantities of soluble chitosan for in vivo delivery where nanoparticles are to be injected at physiological pH values close to the chitosan pK_a of 6.5.

In general, efficient nanoparticle internalization depends on factors such as cell type, physicochemical surface properties of the nanoparticles, and the bio–nano interface.[60] In this report, we demonstrated that LMW-CS nanoparticles were efficiently internalized in multiple cell lines. The uptake efficiency as measured by flow cytometry ranged from 50% (Raw269.7) to 95% (A549 and HEK293), depending on the cell line. Statistical analysis of uptake efficiency intercell lines showed meaningful differences when comparing the A549 and HEK293 (high uptake) to the LS174T and Raw269.7 (medium uptake), indicating a cell-line dependency of chitosan uptake. The cell-line dependency of chitosan nanoparticles uptake was previously suggested to be associated with different endocytic pathways.[81,82] Flow cytometry data

showed LMW-CS nanoparticles to be efficiently internalized to levels similar or higher than commercially available liposomal systems such as DharmaFECT.

Finally, the transfection efficiency of LMW-CS nanoparticles as measured by gene-silencing efficacy was evaluated in two different cell lines: *RecQL1* in LS174T cells and *ApoB* in HepG2 cells. The ability of these chitosan formulations to efficiently silence gene expression reached more than a twofold specific mRNA knockdown; with chitosan 92-10-5 being the most efficient and specific in the LS174T cell line. Other low molecular weight formulations also achieved good levels of gene silencing in the LS174T cell line. Interestingly, chitosan 80-10-10 achieved a high level of silencing with a concomitant increase in silencing when delivering mock siRNA. This intriguing observation is currently under investigation in our laboratory. The chitosan formulation 92-10-5 complexed to ApoB siRNA showed lower target mRNA knockdown in HepG2 when compared to the LS174T cell lines targeted with the RecQL1 siRNA. The silencing efficiency correlated well with uptake efficiency as observed by flow cytometry where chitosan 92-10-5 showed both high uptake and high silencing efficiencies. Despite structural differences between pDNA and siRNA,[46] the chitosan formulation 92-10-5 has shown the highest transfection efficiencies for both siRNA and pDNA to date.[37–41] Taken together, our results show that LWM-CS nanoparticles at low N:P ratios can achieve efficient uptake and gene silencing in vitro, serving as a proof of concept for their use as efficient siRNA delivery vectors in cancer and atherosclerotic animal models. Although in vitro and in vivo performance criteria differ, no consensus on such performances has been established. For in vivo performance, safety remains the major issue, with guidance available from the US Food and Drug Administration for the development of gene and cell therapy products.[83] Therefore, the development of nonviral drug delivery systems for in vivo use should take into account physicochemical criteria, cell-based criteria, and, most importantly, in vivo performance and safety criteria (Table 3). The low molecular weight, low N:P system presented here meets many of these criteria and has already been demonstrated as efficient in vivo for plasmid DNA delivery.[37,41] Thus a complete characterization of the safety and in vivo performance of our LMW-CS system delivering RecQL1 and ApoB targeting siRNA is currently under investigation in animal models of cancer and atherosclerosis.

Acknowledgments

This work was supported by the National Science and Engineering Research Council (NSERC) and by the Groupe de Recherche en Sciences et Technologies Biomédicales of the Fonds de la Recherche en Santé Quebec. We are grateful to Dr Monica Nelea for the ESEM analyses.

Disclosure

The authors declare no conflicts of interest in this work.

References

1. de Fougerolles A, Vornlocher HP, Maraganore J, Lieberman J. Interfering with disease: a progress report on siRNA-based therapeutics. *Nat Rev Drug Discov*. 2007;6(6):443–453.
2. Fire A, Xu S, Montgomery MK, Kostas SA, Driver SE, Mello CC. Potent and specific genetic interference by double-stranded RNA in Caenorhabditis elegans. *Nature*. 1998;391(6669):806–811.
3. Alameh M, Jean M, DeJesus D, Buschmann MD, Merzouki A. Chitosanase-based method for RNA isolation from cells transfected with chitosan/siRNA nanocomplexes for real-time RT-PCR in gene silencing. *Int J Nanomedicine*. 2010;5:473.
4. Bantounas I, Phylactou LA, Uney JB. RNA interference and the use of small interfering RNA to study gene function in mammalian systems. *J Mol Endocrinol*. 2004;33(3):545–557.
5. Castanotto D, Rossi JJ. The promises and pitfalls of RNA-interference-based therapeutics. *Nature*. 2009;457(7228):426–433.
6. Futami K, Kumagai E, Makino H, et al. Induction of mitotic cell death in cancer cells by small interference RNA suppressing the expression of RecQL1 helicase. *Cancer Sci*. 2008;99(1):71–80.
7. Futami K, Kumagai E, Makino H, et al. Anticancer activity of RecQL1 helicase siRNA in mouse xenograft models. *Cancer Sci*. 2008; 99(6):1227–1236.
8. Howard KA, Rahbek UL, Liu X, et al. RNA interference in vitro and in vivo using a novel chitosan/siRNA nanoparticle system. *Mol Ther*. 2006;14(4):476–484.
9. Soutschek J, Akinc A, Bramlage B, et al. Therapeutic silencing of an endogenous gene by systemic administration of modified siRNAs. *Nature*. 2004;432(7014):173–178.
10. Zimmermann TS, Lee AC, Akinc A, et al. RNAi-mediated gene silencing in non-human primates. *Nature*. 2006;441(7089):111–114.
11. Elbashir SM, Harborth J, Lendeckel W, Yalcin A, Weber K, Tuschl T. Duplexes of 21-nucleotide RNAs mediate RNA interference in cultured mammalian cells. *Nature*. 2001;411(6836):494–498.
12. Whelan J. First clinical data on RNAi. *Drug Discov Today*. 2005;10(15): 1014–1015.
13. Corey DR. RNA learns from antisense. *Nat Chem Biol*. 2007;3(1): 8–11.
14. Corey DR. Chemical modification: the key to clinical application of RNA interference? *J Clin Invest*. 2007;117(12):3615–3622.
15. Stein CA. Phosphorothioate antisense oligodeoxynucleotides: questions of specificity. *Trends Biotechnol*. 1996;14(5):147–149.
16. Urban-Klein B, Werth S, Abuharbeid S, Czubayko F, Aigner A. RNAi-mediated gene-targeting throught systemic application of polyethylenimine (PEI)-complexed siRNA in vivo. *Gene Ther*. 2004; 12(5):461–466.
17. Katas H, Alpar HO. Development and characterisation of chitosan nanoparticles for siRNA delivery. *J Control Release*. 2006;115(2): 216–225.
18. Elmen J, Thonberg H, Ljungberg K, et al. Locked nucleic acid (LNA) mediated improvements in siRNA stability and functionality. *Nucleic Acids Res*. 2005;33(1):439–447.
19. Judge AD, Bola G, Lee AC, MacLachlan I. Design of noninflammatory synthetic siRNA mediating potent gene silencing in vivo. *Mol Ther*. 2006;13(3):494–505.
20. Whitehead KA, Langer R, Anderson DG. Knocking down barriers: advances in siRNA delivery. *Nat Rev Drug Discov*. 2009;8(2): 129–138.

21. Bramsen JB, Laursen MB, Nielsen AF, et al. A large-scale chemical modification screen identifies design rules to generate siRNAs with high activity, high stability and low toxicity. *Nucleic Acids Res*. 2009;37(9):2867–2881.
22. Layzer JM, McCaffrey AP, Tanner AK, Huang Z, Kay MA, Sullenger BA. In vivo activity of nuclease-resistant siRNAs. *RNA*. 2004;10(5):766–771.
23. Weyermann J, Lochmann D, Georgens C, Zimmer A. Albumin-protamine-oligonucleotide-nanoparticles as a new antisense delivery system. Part 2: cellular uptake and effect. *Eur J Pharm Biopharm*. 2005; 59(3):431–438.
24. Amarzguioui M, Holen T, Babaie E, Prydz H. Tolerance for mutations and chemical modifications in a siRNA. *Nucleic Acids Res*. 2003; 31(2):589–595.
25. Parrish S, Fleenor J, Xu S, Mello C, Fire A. Functional anatomy of a dsRNA trigger: differential requirement for the two trigger strands in RNA interference. *Mol Cell*. 2000;6(5):1077–1087.
26. Braasch DA, Jensen S, Liu Y, et al. RNA interference in mammalian cells by chemically-modified RNA. *Biochemistry*. 2003; 42(26):7967–7975.
27. Harborth J, Elbashir SM, Vandenburgh K, et al. Sequence, chemical, and structural variation of small interfering RNAs and short hairpin RNAs and the effect on mammalian gene silencing. *Antisense Nucleic Acid Drug Dev*. 2003;13(2):83–105.
28. Reasor MJ, Kacew S. Drug-induced phospholipidosis: are there functional consequences? *Exp Biol Med (Maywood)*. 2001;226(9):825–830.
29. Tousignant JD, Gates AL, Ingram LA, et al. Comprehensive analysis of the acute toxicities induced by systemic administration of cationic lipid:plasmid DNA complexes in mice. *Hum Gene Ther*. 2000; 11(18):2493–2513.
30. Ishida T, Ichihara M, Wang X, et al. Injection of PEGylated liposomes in rats elicits PEG-specific IgM, which is responsible for rapid elimination of a second dose of PEGylated liposomes. *J Control Release*. 2006;112(1):15–25.
31. Judge A, McClintock K, Phelps JR, MacLachlan I. Hypersensitivity and loss of disease site targeting caused by antibody responses to PEGylated liposomes. *Mol Ther*. 2006;13(2):328–337. Epub November 7, 2005.
32. Semple SC, Harasym TO, Clow KA, Ansell SM, Klimuk SK, Hope MJ. Immunogenicity and rapid blood clearance of liposomes containing polyethylene glycol-lipid conjugates and nucleic acid. *J Pharmacol Exp Ther*. 2005;312(3):1020–1026. Epub November 3, 2004.
33. Boeckle S, von Gersdorff K, van der Piepen S, Culmsee C, Wagner E, Ogris M. Purification of polyethylenimine polyplexes highlights the role of free polycations in gene transfer. *J Gene Med*. 2004;6(10):1102–1111.
34. Moghimi SM, Symonds P, Murray JC, Hunter AC, Debska G, Szewczyk A. A two-stage poly(ethylenimine)-mediated cytotoxicity: implications for gene transfer/therapy. *Mol Ther*. 2005;11(6):990–995.
35. Hunter AC, Moghimi SM. Cationic carriers of genetic material and cell death: a mitochondrial tale. *Biochim Biophys Acta*. 2010; 1797(6–7):1203–1209.
36. Al-Dosari MS, Gao X. Nonviral gene delivery: principle, limitations, and recent progress. *AAPS J*. 2009;(4):671–681. Epub October 16, 2009.
37. Jean M, Smaoui F, Lavertu M, et al. Chitosan-plasmid nanoparticle formulations for IM and SC delivery of recombinant FGF-2 and PDGF-BB or generation of antibodies. *Gene Ther*. 2009;16(9): 1097–1110.
38. Lavertu M, Méthot S, Tran-Khanh N, Buschmann MD. High efficiency gene transfer using chitosan/DNA nanoparticles with specific combinations of molecular weight and degree of deacetylation. *Biomaterials*. 2006;27(27):4815–4824.
39. Nimesh S, Thibault MM, Lavertu M, Buschmann MD. Enhanced gene delivery mediated by low molecular weight chitosan/DNA complexes: effect of pH and serum. *Mol Biotechnol*. 2010;46(2):182–196.
40. Thibault M, Nimesh S, Lavertu M, Buschmann MD. Intracellular trafficking and decondensation kinetics of chitosan-pDNA polyplexes. *Mol Ther*. 2010;18(10):1787–1795.
41. Jean M, Alameh M, Buschmann MD, Merzouki A. Effective and safe gene-based delivery of GLP-1 using chitosan/plasmid-DNA therapeutic nanocomplexes in an animal model of Type 2 Diabetes. *Gene Ther*. 2011;18(8):807–816.
42. Howard KA, Kjems J. Polycation-based nanoparticle delivery for improved RNA interference therapeutics. *Expert Opin Biol Ther*. 2007;7(12):1811–1822.
43. Liu X, Howard KA, Dong M, et al. The influence of polymeric properties on chitosan/siRNA nanoparticle formulation and gene silencing. *Biomaterials*. 2007;28(6):1280–1288.
44. de Campos AM, Diebold Y, Carvalho EL, Sanchez A, Alonso MJ. Chitosan nanoparticles as new ocular drug delivery systems: in vitro stability, in vivo fate, and cellular toxicity. *Pharm Res*. 2004;21(5): 803–810.
45. Onishi H, Machida Y. Biodegradation and distribution of water-soluble chitosan in mice. *Biomaterials*. 1999;20(2):175–182.
46. Mao S, Sun W, Kissel T. Chitosan-based formulations for delivery of DNA and siRNA. *Adv Drug Deliv Rev*. 2010;62(1):12–27.
47. Richardson SC, Kolbe HV, Duncan R. Potential of low molecular mass chitosan as a DNA delivery system: biocompatibility, body distribution and ability to complex and protect DNA. *Int J Pharm*. 1999;178(2):231–243.
48. Huang M, Khor E, Lim LY. Uptake and cytotoxicity of chitosan molecules and nanoparticles: effects of molecular weight and degree of deacetylation. *Pharm Res*. 2004;21(2):344–353.
49. Wiegand C, Winter D, Hipler UC. Molecular-weight-dependent toxic effects of chitosans on the human keratinocyte cell line HaCaT. *Skin Pharmacol Physiol*. 2010;23(3):164–170.
50. Ma PL, Buschmann MD, Winnik FM. One-step analysis of DNA/chitosan complexes by field-flow fractionation reveals particle size and free chitosan content. *Biomacromolecules*. 2010;11(3):549–554.
51. Olofsson SO, Boren J. Apolipoprotein B: a clinically important apolipoprotein which assembles atherogenic lipoproteins and promotes the development of atherosclerosis. *J Intern Med* 2005;258(5):395–410.
52. Sharma S, Doherty KM, Brosh RM Jr. Mechanisms of RecQ helicases in pathways of DNA metabolism and maintenance of genomic stability. *Biochem J*. 2006;398(3):319–337.
53. Scaringe SA, Wincott FE, Caruthers MH. Novel RNA synthesis method using 5′-silyl-2′-orthoester protecting groups. *J Am Chem Soc*. 1998;120:11820–11821.
54. Nguyen S, Hisiger S, Jolicoeur M, Winnik FM, Buschmann MD. Fractionation and characterization of chitosan by analytical SEC and ^{1}H-NMR after semi-preparative SEC. *Carbohydr Polym*. 2009;75:636–646.
55. Nguyen S, Winnik FM, Buschmann MD. Improved reproducibility in the determination of the molecular weight of chitosan by analytical size exclusion chromatography. *Carbohydr Polym*. 2009;75:528–533.
56. Lavertu M, Xia Z, Serreqi AN, et al. A validated ^{1}H-NMR method for the determination of the degree of deacetylation of chitosan. *J Pharm Biomed Anal*. 2003;32(6):1149–1158.
57. Skrypina NA, Timofeeva AV, Khaspekov GL, Savochkina LP, Beabealashvilli R. Total RNA suitable for molecular biology analysis. *J Biotechnol*. 2003;105(1–2):1–9.
58. Quong D, Neufeld RJ. DNA protection from extracapsular nucleases, within chitosan- or poly-L-lysine-coated alginate beads. *Biotechnol Bioeng*. 1998;60(1):124–134.
59. Ma PL, Lavertu M, Winnik FM, Buschmann MD. New insights into chitosan-DNA interactions using isothermal titration microcalorimetry. *Biomacromolecules*. 2009;10(6):1490–1499.
60. Nel AE, Madler L, Velegol D, et al. Understanding biophysicochemical interactions at the nano-bio interface. *Nat Mater*. 2009;8(7):543–557.
61. Wu L, Hickson ID. DNA helicases required for homologous recombination and repair of damaged replication forks. *Annu Rev Genet*. 2006;40:279–306.
62. Kawabe T, Tsuyama N, Kitao S, et al. Differential regulation of human RecQ family helicases in cell transformation and cell cycle. *Oncogene*. 2000;19(41):4764–4772.

63. Schaefer JR, Scharnagl H, Baumstark MW, et al. Homozygous familial defective apolipoprotein B-100. Enhanced removal of apolipoprotein E-containing VLDLs and decreased production of LDLs. *Arterioscler Thromb Vasc Biol*. 1997;17(2):348–353.
64. Itabe H. Oxidative modification of LDL: its pathological role in atherosclerosis. *Clin Rev Allergy Immunol*. 2009;37(1):4–11.
65. Gref R, Domb A, Quellec P, et al. The controlled intravenous delivery of drugs using PEG-coated sterically stabilized nanospheres. *Adv Drug Deliv Rev*. 1995;16:215–233.
66. Bivas-Benita M, Romeijn S, Junginger HE, Borchard G. PLGA-PEI nanoparticles for gene delivery to pulmonary epithelium. *Eur J Pharm Biopharm*. 2004;58(1):1–6.
67. Panyam J, Labhasetwar V. Biodegradable nanoparticles for drug and gene delivery to cells and tissue. *Adv Drug Deliv Rev*. 2003; 55(3):329–347.
68. Guy J, Drabek D, Antoniou M. Delivery of DNA into mammalian cells by receptor-mediated endocytosis and gene therapy. *Mol Biotechnol*. 1995;3(3):237–248.
69. Desai MP, Labhasetwar V, Amidon GL, Levy RJ. Gastrointestinal uptake of biodegradable microparticles: effect of particle size. *Pharm Res*. 1996;13(12):1838–1845.
70. Seymour LW. Passive tumor targeting of soluble macromolecules and drug conjugates. *Crit Rev Ther Drug Carrier Syst*. 1992; 9(2):135–187.
71. Jean M, Alameh M, De Jesus D, et al. Chitosan-based therapeutic nanocomplexes for combination gene therapy and gene silencing of in vitro cell lines relevant to type 2 diabetes. *Eur J Pharm Sci*. 2011; 45(1–2):138–149. Epub November 9, 2011.
72. Chithrani BD, Chan WC. Elucidating the mechanism of cellular uptake and removal of protein-coated gold nanoparticles of different sizes and shapes. *Nano Lett*. 2007;7(6):1542–1550.
73. Chithrani BD, Ghazani AA, Chan WC. Determining the size and shape dependence of gold nanoparticle uptake into mammalian cells. *Nano Lett*. 2006;6(4):662–668.
74. Verma A, Stellacci F. Effect of surface properties on nanoparticle-cell interactions. *Small*. 2010;6(1):12–21.
75. Liu W, Sun S, Cao Z, et al. An investigation on the physicochemical properties of chitosan/DNA polyelectrolyte complexes. *Biomaterials*. 2005;26(15):2705–2711.
76. Erbacher P, Zou S, Bettinger T, Steffan AM, Remy JS. Chitosan-based vector/DNA complexes for gene delivery: biophysical characteristics and transfection ability. *Pharm Res*. 1998;15(9):1332–1339.
77. Danielsen S, Strand S, de Lange Davies C, Stokke BT. Glycosaminoglycan destabilization of DNA-chitosan polyplexes for gene delivery depends on chitosan chain length and GAG properties. *Biochim Biophys Acta*. 2005;1721(1–3):44–54. Epub November 2, 2004.
78. Köping-Höggård M, Mel'nikova YS, Vårum KM, Lindman B, Artursson P. Relationship between the physical shape and the efficiency of oligomeric chitosan as a gene delivery system in vitro and in vivo. *J Gene Med*. 2003;5(2):130–141.
79. Gao S, Dagnaes-Hansen F, Nielsen EJ, et al. The effect of chemical modification and nanoparticle formulation on stability and biodistribution of siRNA in mice. *Mol Ther*. 2009;17(7):1225–1233.
80. Ji AM, Su D, Che O, et al. Functional gene silencing mediated by chitosan/siRNA nanocomplexes. *Nanotechnology*. 2009;20(40):405103.
81. Bishop NE. An Update on Non-clathrin-coated Endocytosis. *Rev Med Virol*. 1997;7(4):199–209.
82. Huang M, Ma Z, Khor E, Lim LY. Uptake of FITC-chitosan nanoparticles by A549 cells. *Pharm Res*. 2002;19(10):1488–1494.
83. Center for Biologics Evaluation and Research, US Food and Drug Administration. *Guidance for Industry: Considerations for Plasmid DNA Vaccines for Infectious Disease Indications*. Rockville, MD; 2007. Available from: http://www.fda.gov/BiologicsBloodVaccines/GuidanceComplianceRegulatoryInformation/Guidances/Vaccines/ucm074770.htm. Accessed January 1, 2012.
84. Center for Biologics Evaluation and Research. *Guidance for Industry: Considerations for Plasmid DNA Vaccines for Infectious Disease Indications*. Rockville, MD: US FDA; 2007. Available from: http://iccvam.niehs.nih.gov/SuppDocs/FedDocs/FDA/FDA_plasdnavac.pdf. Accessed February 23, 2012.
85. Center for Biologics Evaluation and Research. *Guidance for FDA Reviewers and Sponsors: Content and Review of Chemistry, Manufacturing, and Control (CMC) Information for Human Gene Therapy Investigational New Drug Applications (INDs)*. Rockville, MD: US FDA; 2008. Available from: http://www.fda.gov/downloads/BiologicsBloodVaccines/GuidanceComplianceRegulatoryInformation/Guidances/CellularandGeneTherapy/ucm078694.pdf. Accessed February 23, 2012.
86. US Pharmacopeial Convention. Gene therapy products. In: Second Supplement to *USP 34-NF 29*. Rockville, MD: United States Pharmacopeial; 2011:5135–5158.